DESIGNING A NEW BELL-TYPE PRIMARY AIR NOZZLE FOR A LARGE-SCALE CIRCULATING FLUIDIZED BED BOILERS

Mustafa Metin Çam [a*], Cenk Çelik [b], Mansour Al Qubeissi [c] Hakan Serhad Soyhan [d,e],

[a] TUBITAK Marmara Research Center, Gebze, Kocaeli, 41470, Turkey
[b] Department of Mechanical Engineering, Umuttepe Campus, Kocaeli University, Kocaeli, 41040 Turkey
[c] Faculty of Engineering, Environment and Computing, Coventry University, Coventry CV1 2JH, United Kingdom
[d] Department of Mechanical Engineering, Engineering Faculty, Esentepe Campus, Sakarya University, Sakarya 54050, Turkey
[e] Team-SAN Co., Technological Development Centre, Sakarya University, 54187, Sakarya, Turkey

_____

Abstract

The design of energy efficient engineering systems is crucial for sustainable operation when economic and environmental consequences are considered. Circulating Fluidized Bed (CFB) boilers, which are among the major contributors to world electricity production, are still increasing in numbers and unit sizes. Primary air nozzles are key components of CFB boilers that may decrease energy consumption and increase energy efficiency, and they need to be carefully designed. There are certain types of nozzles commonly used in the air distribution grate, but even minor design improvements on the nozzle can significantly decrease the pressure loss. This work is about optimizing the bell-type primary air nozzle used in the Turkish lignite-fired ÇAN Thermal Power Plant (CTPP), which has two 160 MWe CFB boilers, through computational fluid dynamics (CFD). Initially, the bell-type nozzle was designed newly by changing the inner head holes geometry. After that, the nozzle geometry was optimized by changing the orifice size and angle to decrease the pressure drop, increase the orifice velocity outlet, and flow uniformity through CFD simulations. With the optimum nozzle geometry, the velocity at the outlet orifices was increased, and a decrease of 2.86 kPa was achieved in the total pressure loss. Furthermore, when the nozzle orifices were designed downwardly with an angle of 105°, pressure drop across the nozzle decreased by 7.6%, and the uniformity index increased by 2 % at the outlet orifices. Using the bell-type primary air nozzle, which is newly designed, in the CTPP boiler not only

---

[*] Corresponding author. Tel.:+90 262 6773110; fax: +90 262 6412309
E-mail address: _metin.cam@tubitak.gov.tr_ (M.M.Çam).

1

will save 2.26 GWh/year of energy consumption but also minimize the backflow risk in the boiler operation.

Keywords: Nozzle, Circulating fluidized bed, Computational fluid dynamics, Optimization.

Nomenclature	
CFB	Circulating fluidized bed
CFD	Computational fluid dynamics
CTPP	ÇAN Thermal Power Plant
C_μ	viscosity constant
$C_{1\epsilon}$	k-ε model constant [1,44]
$C_{2\epsilon}$	k-ε model constant [1,92]
d_o	Orifice diameter
g	gravity [m/s^2]
G_k	Generation of turbulent kinetic energy
k	turbulent kinetic energy [m^2/s^2]
N_o	Number of orifice
p_1	fan inlet pressure [kPa]
p_2	fan outlet pressure [kPa]
U_0	orifice velocity outlet [m/s]
v_1	flow rate [m^3/s]
Δp	pressure drop across the nozzle [kPa]
ρ_o	density of gas at the orifice outlet [kg/m^3]
β	angle of orifice
ε	turbulent dissipation rate [m^2/s^2]
σ_k	turbulent Prandtl constant
σ_ϵ	turbulent Prandtl constant
μ_t	turbulence viscosity [Ns/m^2]
$w_{s,ideal}$	ideal shaft work [W]
γ	specific heat
η_f	fan efficiency
η_m	motor efficiency

2

η_b	belt efficiency.

1. Introduction

Fluidized bed technology is one of the most suitable combustion systems in terms of bringing lignite to energy production [1]. The most important advantage of fluidized bed combustion technology is that it enables low-calorific solid fuels such as lignite and bio-waste to be combust in high efficiency and low NOx and SO2 emission values, especially compared to the traditional pulverized combustion system [2,3]. Fluidized bed combustion system consist of three groups according to their working principle. These are bubbling fluidized beds (BFB), circulating fluidized beds (CFB) and pressurized fluidized beds (PFB) [4]. CFB is the most widely used technology among them [5]. In [6], it was stated that CFB boiler technology has been developed considerably over the past 20 years, its installed power capacities were increased up to 600 MWe in a single unit, and its use has increased rapidly in the world.

In CFB boilers, about 40-60% of the total combustion air, which is primary air, is fed from the bottom part of the combustion chamber by the air distributor grate and the remaining air (secondary air) is fed from an upper level of the air distributor grate. With the air fed from the distributor grate, the bed material becomes fluidizing and moves upwards. Coarse ash falls down along the sidewalls, while other materials separate from each other in cyclones. Then, relatively big materials return to the combustion chamber via fluidization air from the ash return legs and cycle finish [7].

CFB boiler's air grate main purpose is to distribute the primary air uniformly in the combustion chamber [8]. Therefore, its design has great importance in terms of combustion efficiency in the CFB boilers [9]. Due to the defects of distributor grate design, many problems may be occurring in the boiler operation. The common problems are decreasing in combustion efficiency due to the nonuniform-unstable fluidization across the dense bed, increasing pressure drop thus rising internal energy demand,

4

plugging and breaking, backflow of bed material into the windbox, shortening service life due to erosion of the nozzles and abrasion of solid particles in the bed [10].

There are three different types of air distributor plate used in the fluidized bed boilers. These are perforated plate, nozzle and scatter tube. Nozzles is more safety design and commonly used as an air distributor in CFB boilers [11]. The minimum required pressure drop across the air distributor may vary depending on the nozzles structure, windbox geometry and characteristic feature of the CFB boiler [12].

Numerous correlations improved and verified before regarding the minimum pressure required for fluidized bed systems are available in the literature. The widely accepted minimum required pressure loss for large-scale CFB boilers is of 30% of the pressure difference across the fluidized bed [13]. At the same time, while the low-pressure drop in the nozzle reduces the resistance against the backflow of the bed material into the windbox, the high-pressure drop increases the internal energy consumption due to the fan load. Internal energy consumption is a major cost factor in any process using fluidized beds and can sometimes eliminate the advantages of this type of combustion systems [14].

In addition, the air velocity at the nozzle orifice outlet directly affects the pressure drop and fluidization. While the air velocity less than 30 m/s at the nozzle orifice outlet is generally considered safe it is stated that it is risky if the orifice outlet gas velocity is greater than 90 m/s [15].

There are rather limited and specific studies about the primary air nozzle used in CFB boilers in the literature, but a few experimental and numerical studies about improving nozzle geometry to decrease pressure drop and increase uniformity in the nozzle airflow pattern. For instances, Yang *et al.* [16], and Huang *et al.* [17] developed a

5

new type of nozzle design sensitive to flow rate in their studies. By performing the performance tests in the experimental setup of the nozzle, the pressure drop characteristic curve depending on the flow rate was obtained. They stated that the new type nozzle has 60% less pressure drop compared to the standard bell-type air nozzle. However, they stated that the resistance of the nozzle against the main problems such as unbalanced air distribution, backflow to windbox, and material wear should be investigated with additional experimental and CFD analysis. In another study, Mirek [18] purposed to develop a new type of nozzle geometry through CFD analysis and an experimental approach for a 235 MW$_e$ CFB boiler. He designed the new type of nozzle geometry by targeting two basic criteria. The first criteria was to obtain a uniform gas velocity profile within the nozzle. The second criteria was to perform a geometric design that would resist the reverse direction of flow in the event of strong negative pressure. Thus, with the novel nozzle design achieved a 545 Pa in pressure drop improvement compared to the existing arrowhead nozzle in the CFB boiler. Omer and Weng [19] measured the pressure drop of each of 500 nozzles in a 105MWt CFB boiler and making the bed pressure drop map out in their study. Accordingly, the effect of non-uniform primary air distribution on the solid-gas mixture throughout the boiler was investigated by CFD modeling. It was stated that nozzles are subject to excessive wear and clogging, often in certain areas on the large-scale boiler bottom of the bed, causing non-uniform primary air distribution. Mirek and Klajny [20] stated that the backflow of the bed material into the air plenum was eliminated with the new type of nozzle developed instead of the arrow type nozzle used in the 466 MWe CFB boiler. The number of outlet orifices, which were two in the existed nozzle, were four in the new type of nozzle and obtained uniform air distribution in the nozzle by enhancing the inner geometry of the nozzle through CFD analysis. As a result of this study, while increasing the velocity

6

outlet of the nozzle orifice from 64 m/s to 90 m/s, pressure drop and internal energy demand were the same as in the old primary air distribution system. In [21], the thermal efficiency has been increased from 86.4% to 91.8% using the new bell-type nozzle for a CFB boiler of steam capacity 220 tons/hour. The authors improved the novel bell-type nozzle geometry through CFD analysis. Hence, they provided an 18.9% improving in pressure drop compared to a conventional bell-type nozzle and making 66% upgrading in flow uniformity, and also preventing bed material back-flow by designing the orifices 30° downwards. Huang *et al.* [22] improved the design of the bell-type nozzle used in the air distributor of a 480 t/h CFB boiler through CFD analysis. Within the scope of the design, the risk of clogging was reduced by giving a special shape to the nozzle orifice outlet and thus the service life was extended.

In the abovementioned literature, there is research on the enhancement of the nozzle design and its effects on the CFB boilers. These studies are rather limited in the literature. It has been seen that there is no study in the literature on the optimization of nozzle geometry, the share of nozzle-induced pressure loss in energy consumption on a CFB boiler unit, and the effect of the angle of the nozzle orifices on the pressure drop. It is also emphasized in [23] that the nozzle design can differ depending on the CFB boiler characteristic and the engineering approach of the designer.

In this work, the bell-type primary air nozzle used in the 160 MWe CTPP CFB boiler is investigated. Firstly, the nozzle is numerically modeled using commercial CFD software from ANSYS Fluent®. Because, recent developments in CFD have enabled the modeling of complex and high turbulent flow in the nozzle interior and elaborately observing the effects of changes in nozzle geometry on pressure and velocity distributions. Thus, CFD simulation helps engineers to precise design of nozzle geometry for

7

less time and less cost. CFD simulation method is preferred to optimize nozzle geometry in this research. The model is validated by comparing the data measured in the CFB boiler unit under the same operational conditions. The effect of pressure drop in the nozzle on the internal energy consumption of the plant is calculated and examined. In order to minimize the pressure drop, the bell-type primary air nozzle geometry was designed newly by opening 8 slots (instead of the original 16 holes) on the inner head in the model. Also, the effect of orifice number and diameter variations on total pressure drop and orifice velocity outlet are investigated in the newly designed nozzle model. To optimize newly designed nozzle model, crucial constraints, like minimum required pressure drop and maximum velocity outlet at the nozzle for large-scale CFB boilers, are used as reference points. Furthermore, to increase the flow uniformity at the outlet of the nozzle model, contours of the total pressure and velocity distribution at the various numbers of orifices, their diameters, and angles are examined, using the CFD modelling. Hence, the optimum orifice diameter and angle have been determined based on the number of orifices.

As seen in literature, CFD approach has been used in several works [24,25]. In what follows, the property of CTPP Unit I and methodology are presented in Section 2, including 3D airflow volume, study of mesh independence, physical properties of CFD model, and model validation. The optimization study of the bell-type primary air nozzle is discussed in Section 3, including the effects of pressure drop, effects of the newly designed nozzle head, effects of the orifice number and diameter, effect of the orifice angle. The results obtained from observations are summarized in Chapter 4. Finally, the contribution of the newly designed optimum nozzle to the CTPP in terms of electrical power consumption is presented in Section 5.

8

2. Methodology

2.1 System definition

Çan Thermal Power Plant (CTPP) consists of two units, Unit I and Unit II the same technical specifications. The total electric power of units is 160 MWe capacity. *Unit I* is taken as a reference in this study. Unit I measure 50 m in height, 7.9 m in width, and 14.5 m in depth CFB boiler with a steam generation capacity of 462 tons/hour [26]. Further details of the CTPP boiler as seen in **Fig. 1.**
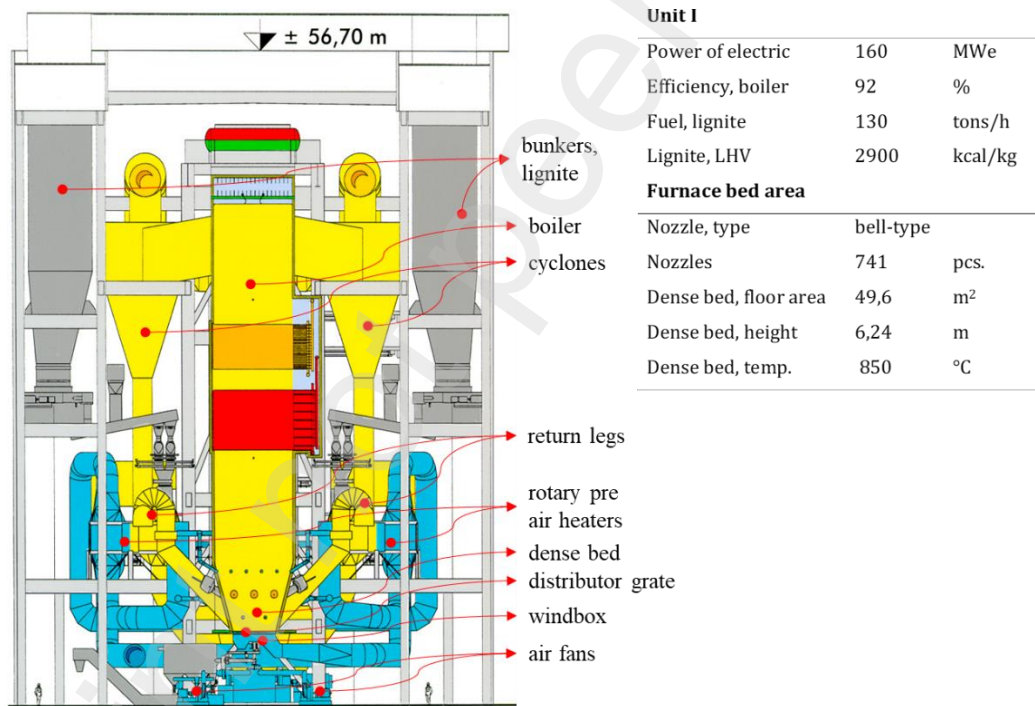

Unit I		
Power of electric	160	MWe
Efficiency, boiler	92	%
Fuel, lignite	130	tons/h
Lignite, LHV	2900	kcal/kg
Furnace bed area		
Nozzle, type	bell-type	
Nozzles	741	pcs.
Dense bed, floor area	49,6	m²
Dense bed, height	6,24	m
Dense bed, temp.	850	°C

Fig. 1. Schematic diagram and characteristic parameters of the CFB boiler 160 MWe in CTPP.

The dense bed zone of the CFB boiler is conical in shape and expands upwards, its height 6.24 meters. Approximately 43% of the combustion air fed to the boiler is primary air and is fed from the bed floor. The remaining combustion air is secondary air fed to the system by air ducts at 2 levels, 1 and 5 meters respectively above the bed

9

floor. While the unit is operating at 100 % capacity, the fresh air taken by the primary air fans first passes through the rotary type heat exchanger and the temperature of the air is increased about 287 °C. Then it transfers to the wind box located in the bottom part of the CFB boiler. Finally, primary air 69.2 kg/s feed to the CFB boiler through 741 nozzles located at the bottom of the combustion chamber as seen in **Fig. 2.**[27]**.**
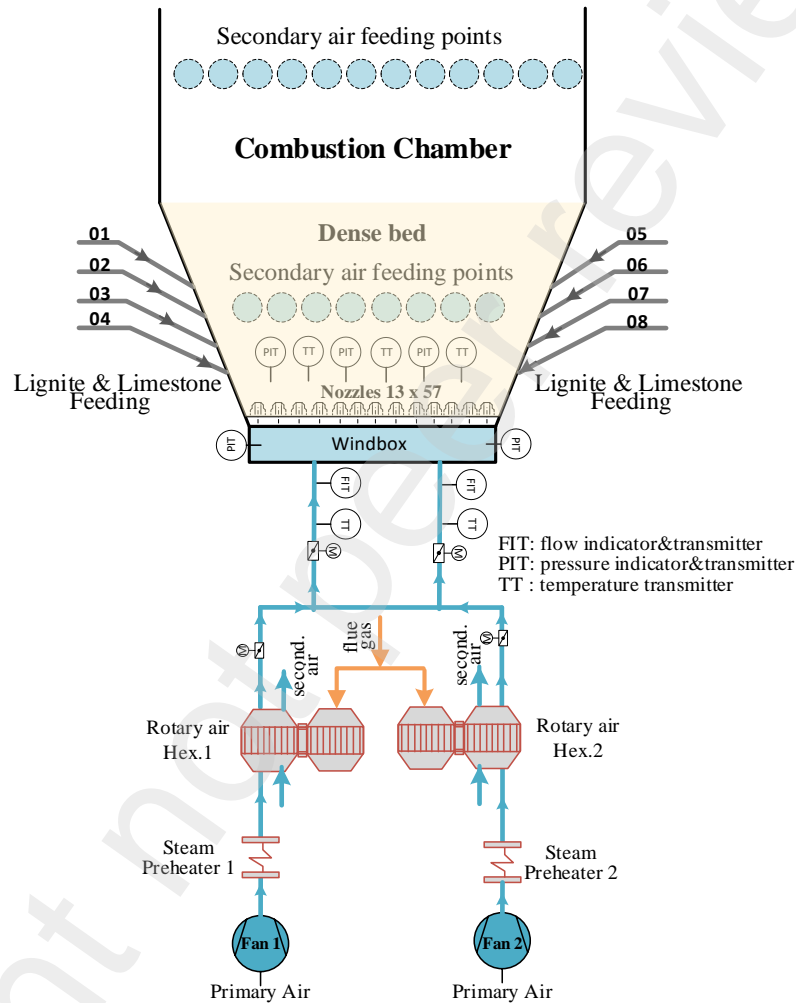
Fig. 2. Schematic diagram of the primary airflow in the CTPP boiler bed zone.

The bell-type primary nozzles used for primary air distribution in CTPP boiler consist of three essential parts that can screw to each other. First part is a pipe connected to the bottom of the bed, 73 mm in diameter. Second part is inner head, 70 mm in diameter. Third part is cover, 150 mm in diameter. The inner head of the nozzle has 16

10

holes at two levels with a diameter of 12 mm, and there are eight orifices with a diameter of 20 mm on the cover as shown in **Fig.3.**

(a)
Schematic view of the bell-type nozzle head

(b)
Configuration of the nozzle in CTPP boiler bed floor zone
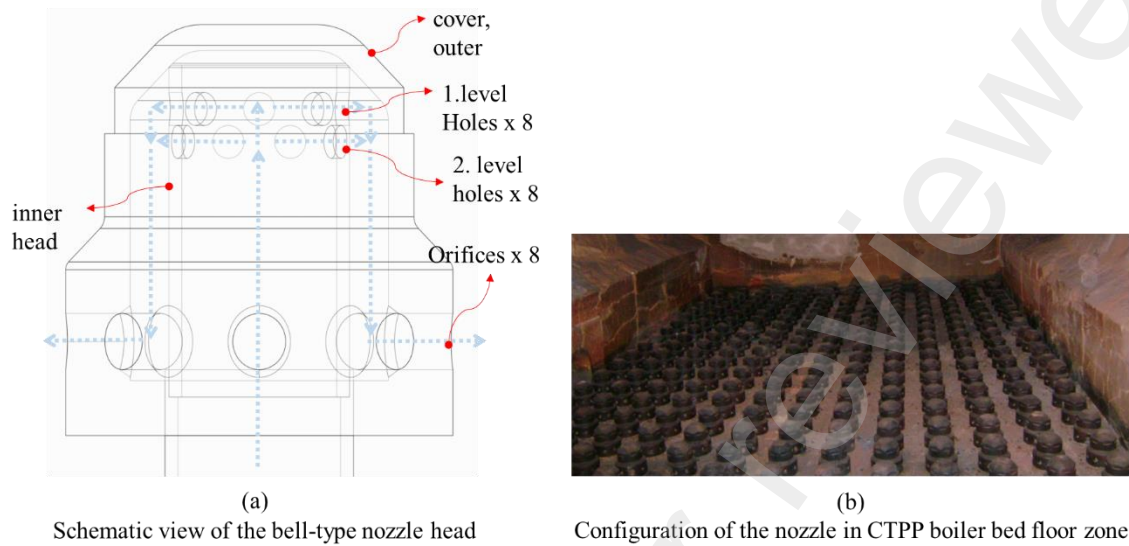
Fig. 3. Schematic and configuration view of the bell-type nozzle in CTPP boiler.

2.2 CFD Model

The bell-type nozzle was firstly drawn in 3D CAD software. After that, the 3D air-flow volume of the nozzle was generated. Then, boundary layers were defined such as mass flow inlet, pressure outlet, fluid, and wall surfaces on the airflow volume as given in **Fig.4.** Finally, this nozzle airflow volume was used in the FLUENT meshing tool for the meshing study.

11
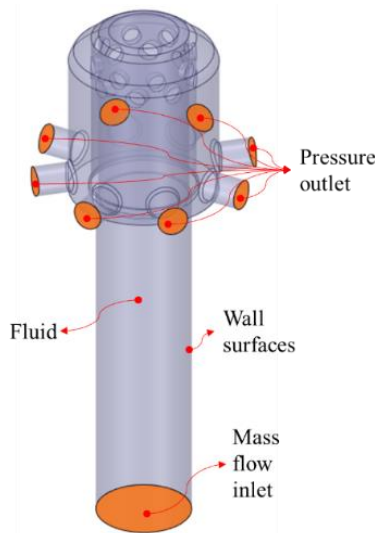
Fig. 4. Boundary definitions in the nozzle airflow volume.

The effect of the mesh numbers at the nozzle flow volume on the total pressure drop is as given in **Fig. 5.** Accordingly, when the mesh number was increased from 172322 to 638903 in the model, the pressure drop increases by 10%, when it was increased to 1089753, the pressure drop increases by 7%, and when it was increased to 1753803, the pressure drop increases by 0.7%. After that in the analyzes performed with finer mesh numbers such as 3246063 and 7460591, it has been observed that the pressure drop changed only by 0.1%. Depending on the computer hardware features, the numerical solution times increase with the increase in the number of mesh in the model. When the numerical solution time and the rate of change in pressure drop is considered the number of 1753803 mesh elements might be acceptable for this study. For this reason, approximately this mesh number was taken as reference in all other numerical analyzes for nozzle optimization studies.

12
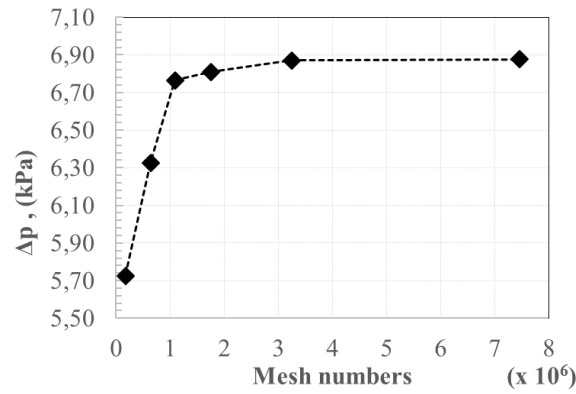
Fig. 5. Mesh independence study of the bell-type nozzle.

In the meantime, the polyhedral mesh was used in this mesh independence study because of providing good accuracy in a shorter time [28]. Inflation layer meshing was also applied to the boundary layer region with ten layers to capture the flow separation and pressure drop with sufficient number of polyhedral mesh elements shown in **Fig. 6.**
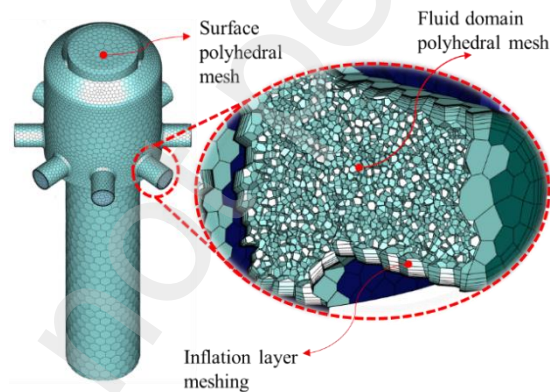

Fig. 6. Polyhedral meshing of the flow volume with ten inflation layers around orifices.

2.3 Physical properties of the CFD model

Reynolds-Averaged Navier-Stokes (RANS) an equation was computed through AN-SYS FLUENT® solver based on the finite volume method. In the RANS approach, different mathematical models are used to calculate the mixing and diffusion flow caused by

13

unsteady turbulent eddies [29]. k–ε model has been generally utilized for the estimation of turbulence was selected because of the capability and convincing results in the nozzle [30]. k–ε model can be formulated with the equations given below, and the turbulence kinetic energy (k), turbulence dissipation rate (ε) can be calculated from these equations. At this equations, Gk represents the turbulent kinetic energy produced by the main velocity gradient and σk, σϵ are the turbulent Prandtls numbers. The model constants used in this equation are $C_{1\epsilon} = 1,44$, $C_{2\epsilon} = 1,92$, $σ_k = 1,0$, $σ_k = 1,3$.

$$\nabla\rho k = \nabla \cdot \left[\left(\mu + \frac{\mu_t}{\sigma_k} \right) \cdot \nabla k \right] + G_k - \rho\varepsilon \tag{1}$$

$$\nabla\rho\varepsilon = \nabla \cdot \left[\left(\mu + \frac{\mu_t}{\sigma_\varepsilon} \right) \cdot \nabla\varepsilon \right] + C_{1\varepsilon}\frac{\varepsilon}{k}G_k - C_{2\varepsilon}\rho\frac{\varepsilon^2}{k} \tag{2}$$

Turbulent viscosity is expressed by the equation given below.

$$\mu_t = \rho C_\mu \frac{k^2}{\varepsilon} \tag{3}$$

The difference of the Realizable k–ε model from the Standard and RNG k–ε model is that in turbulent viscosity balance, the C_μ coefficient is variable, not constant. The realizable k–ε model is suitable for flows at boundary conditions under strong pressure gradients and flows with separation and recombination [31].

In the solution of the nozzle numerical model, 3D, time-independency, viscous flow and realizable k–ε turbulence model was set. As near-wall, mesh was fine enough to be able to resolve the viscous sublayer so the enhanced wall treatment was used for the correct solution [32]. Defined in the FLUENT solver that the flow rate entrance the nozzle is 0.0934 kg/s at the nominal load. In the model, air was selected as the fluid and

14

air properties were entered temperature at 287° C, density ρ_a = 0.632 kg/m³ and dynamic viscosity μ_a = 2.89E-05 Pa.s. Nozzle inlet section, "mass flow inlet" outlet sections, "pressure outlet" and all other surfaces were defined in the model as wall boundary condition. In the model, the hydraulic diameter was D and the turbulence density was estimated with values of 4.6%. The numerical algorithm was used Coupled. The second-order discretization was utilized in that it presents higher-order accuracy, especially for complex flows involving separation.

Additionally, to evaluate the uniformity of the flow fields at the orifices of the nozzle, the velocity uniformity index was utilized as follows;

$$\gamma_a = \frac{\sum_{i=1}^{n}[(|u_i - \overline{u_a}|A_i)]}{2|\overline{u_a}|\sum_{i=1}^{n}A_i} \tag{4}$$

where

$$\overline{u_a} = \frac{\sum_{i=1}^{n}u_i A_i}{\sum_{i=1}^{n}A_i} \tag{5}$$

Here, γ_a is the area-weighted uniformity index. n is the total number of outlet positions. u_i is the velocity at the i_th position, and $\overline{u_a}$ is the mean of the velocities. The value of γ_a is between 0 and 1, $\gamma_a = 1$ shows an excellent uniform distribution [33].

2.4 Validation of the CFD model

Within the scope of on-site measurements in CTPP boiler, pressure measurements were conducted at the inlet and outlet of the boiler's grate plate to determine the pressure drop due to the nozzles. Meanwhile, the boiler was running at full load, the primary air temperature in the windbox was about 287 °C and the temperature at the bottom of the combustion chamber was about 850 °C. The average one-minute differential pressure measurements at the nozzle inlet and outlet of the bed area are given

15

in **Fig. 7.** As most of the CFB boiler operating parameters affect the pressure at the bed area, high fluctuations occur in the pressure drop values. For this reason, measurements were conducted for 2 hours in stable boiler full load conditions and the pressure drop was found to be approximately 6.8 kPa on average due to bell-type nozzle. In the boiler operation depending on the unit-working load, the total primary airflow rates are 69.2 kg/s at 100% load, 58.91 kg/s at 85% load, and 41.5 kg/s at 50% and lower and distribute uniformly among the 741 nozzles was assumed. The characteristic working curve of the existed bell-type nozzle was derived through CFD analysis under the airflow rates corresponding to boiler loads. Accordingly, the effect of the inlet airflow rate on the pressure drop and orifices velocity outlet is given in **Fig. 8.**
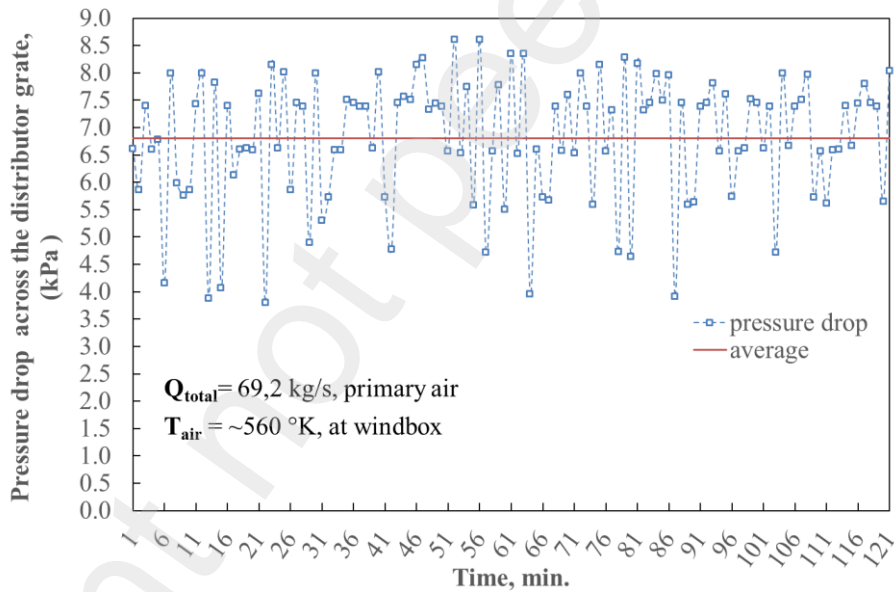
Fig.7. Variation and average of total pressure drop across the nozzles in the CTPP boiler.
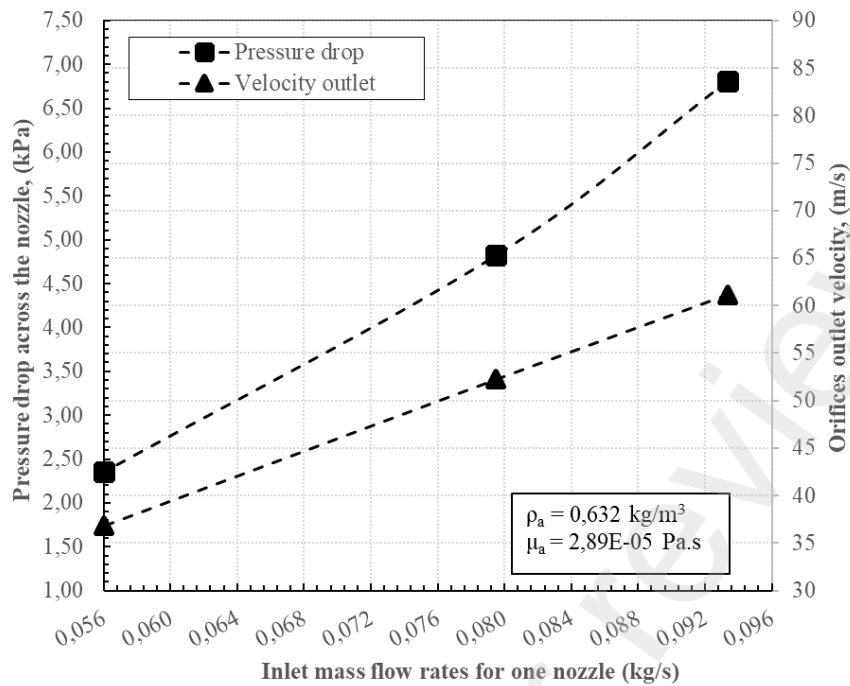
16

Fig. 8. Characteristic curve of the existed bell-type nozzle.

Finally, it has been shown that the average pressure drop in the primary distribution nozzle grid obtained from on-site measurements under the same temperature and mass flow rates at the CTPP boiler operating full load validated the pressure loss value of 6.8 kPa obtained through CFD analysis.

3. Discussion

3.1 Effects of the pressure drop

Atmospheric air taken by the fans is pressurized and passed through the preheaters on two separate lines and is heated to approximately 286°C. The airflow rate heated at full load is about 249 t/h and fed into the windbox under the boiler and then into the dens bed with distributor grid nozzles. Then the primary air is discharged from the chimney, passing through the combustion chamber, first pass, second pass and filters. In order to complete this process in CTPP boiler operation, the gauge pressure of the air at the fan outlet should be 20.2 kPa. The following equations are used to calcu-

17

late the shaft work to compress each kilogram of air in the adiabatic-reversible (isentropic) process when neglecting the kinetic and potential energy effects [14]. The constants used in this equation are $\gamma=1{,}4$, $\eta_f = 0{,}58$, $\eta_m = 0{,}92$ and $\eta_b = 0{,}93$.

$$p_2 - p_1 = \Delta p_b + \Delta p_d + \Delta p_{\text{cyclones and filters}} \tag{6}$$

$$-w_{s,ideal} = \int_{p_1}^{p_2} \frac{dp}{\rho g}, [j/kg] \tag{7}$$

$$-w_{s,ideal} = \frac{\gamma}{\gamma - 1} p_1 v_1 \left[\left(\frac{p_2}{p_1} \right)^{\frac{\gamma-1}{\gamma}} - 1 \right], [W] \tag{8}$$

$$-w_{s,ideal} = \frac{\gamma}{\gamma - 1} p_2 v_2 \left[1 - \left(\frac{p_1}{p_2} \right)^{\frac{\gamma-1}{\gamma}} \right], [W] \tag{9}$$

$$-w_{s,actual} = \frac{-w_{s,ideal}}{\eta_f \, x \, \eta_m \, x \, \eta_b} \tag{10}$$

Accordingly, the required fan power to increase the pressure of 249 t/h air flow by 20.2 kPa is calculated as approximately 2068 kW.

The average value of pressure drop across the nozzle is 6.8 kPa. It was determined that 35% of the pressure loss in the primary airline occurs in the air distributor nozzles. One unit was assumed to operate 7500 hours per year excluding planned maintenance. In this case, the energy consumption in primary fans is 15.5 GWh/year. This value corresponds to approximately 16.3% of the total internal energy demand in the unit. As a result of the pressure loss in the primary air distributor nozzle system, the energy consumption is realized as 5.45 GWh/year. With this energy consumption, it has a share of 5.73% of the total internal energy consumption. The effect of the pressure loss in the nozzle on the fan power consumption is given in **Fig. 9.** Accordingly, with 1 kPa decrease in nozzle pressure drop, it will reduce the energy consumption in primary fans by 4.65% and, save 720,667 kWh/year of electricity consumption.
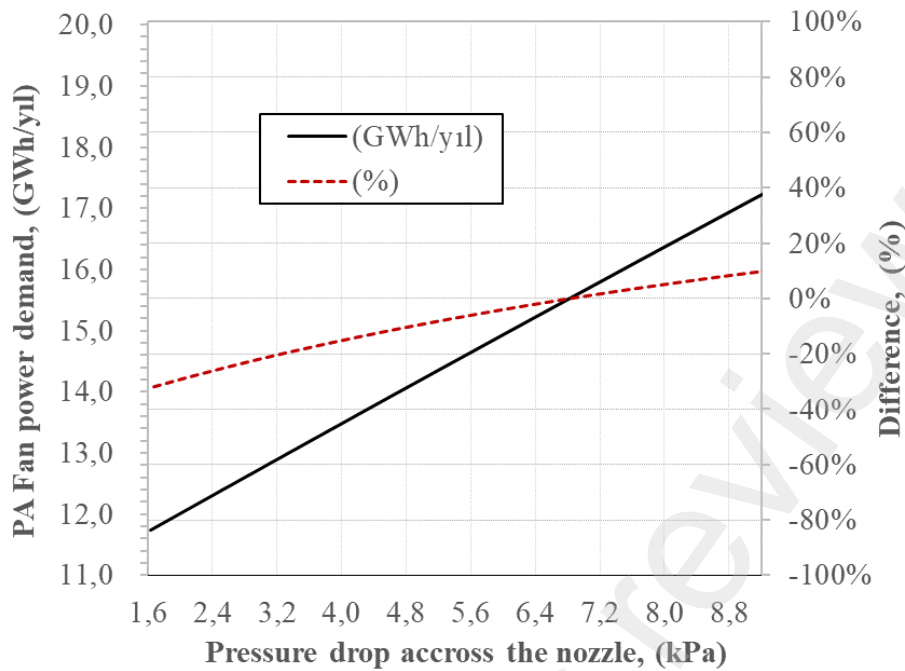
18

Fig. 9. Variation of fan power consumption regarding pressure drop across the nozzle.

3.2 Effects of the newly designed nozzle head

Design of the inner head holes of the bell-type air nozzle used in the CTPP boiler cause high velocity field and turbulence which increase the pressure drop in the nozzle. Therefore, the inner head holes geometry has been changed to reduce the pressure drop at the nozzle and improve the velocity field in this study. Thus, the inner head of the nozzle is newly designed by opening 2x4 slots at 2 levels, 39 mm length and 12 mm diameter instead of 16 holes as seen in **Fig. 10.** After the airflow volume was extracted from the 3D newly designed solid model, performing mesh study and then pressure and velocity parameters were obtained through the CFD analysis.
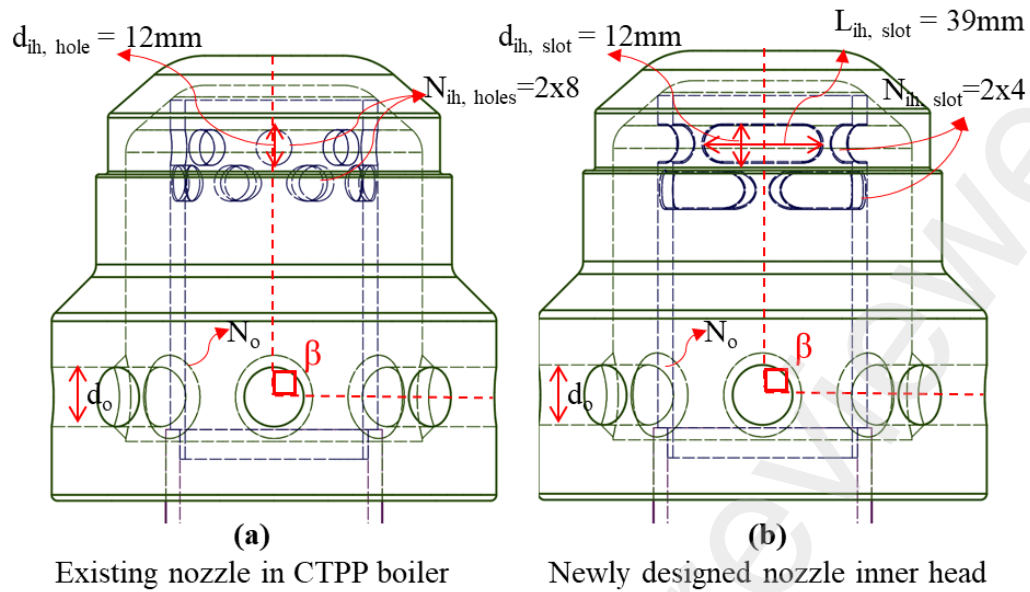
19

Fig. 10. Geometric view of the existed and newly designed bell-type nozzle.

As a result of CFD analysis, a comparative view of the pressure and velocity field contours of existing and newly designed nozzle models are given in **Figs. 11. and 12.** Accordingly, when the total pressure distribution contour is investigated, it is seen that pressure at the inner head of the bell-type air nozzle used in CTPP boiler is around 6.8 kPa. At the same time, it is seen that as the flow progresses from the nozzle arms to the orifice outlet, the pressure decreases and becomes zero at the orifice outlet. Additionally, it was determined that the pressure was very low in the upper wall of the orifice and in the near region. On the other hand, in the newly designed nozzle, the total pressure decreased by 2.9 kPa with the decrease of flow velocities at the outlet of the inner head slots.
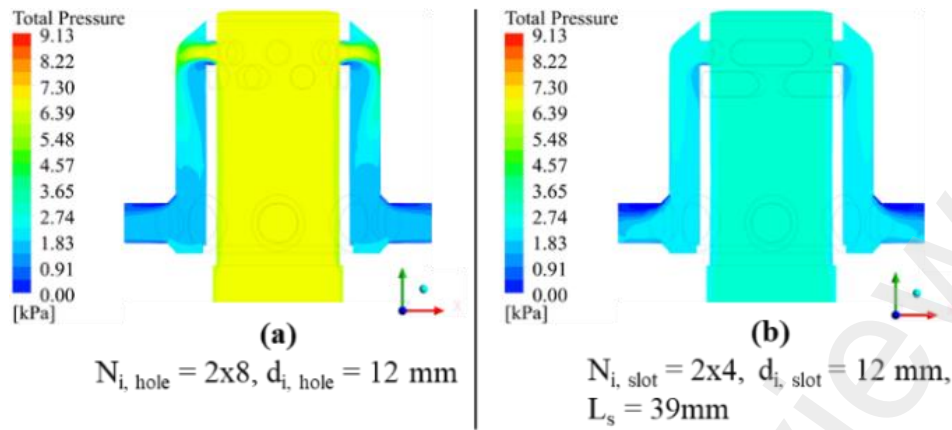
20

Fig. 11. Contours of total pressure distribution (a) existing nozzle in CTPP Boiler (100% load); (b) newly designed nozzle model (100%load).
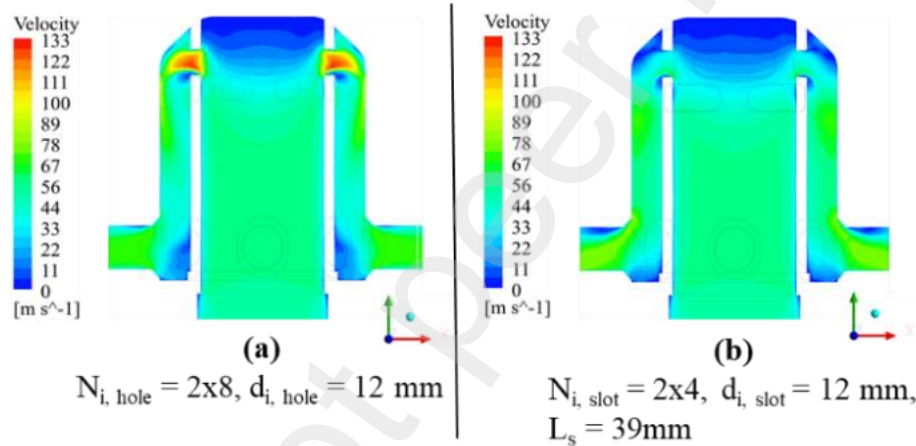

Fig. 12. Contours of velocity distribution (a) existing nozzle in CTPP Boiler (100% load); (b) newly designed nozzle model (100%load).

When the velocity field contour is examined, it has been determined that the flow velocity of the CTPP boiler's nozzle is around 129 m/s at the holes of inner head exit, while this value has decreased to 55 m/s in the new model. This resulted in a significant decrease in pressure loss. In the meanwhile, flow velocities are averaged 61 m/s at the orifice outlet of both nozzles.

The dead zone was relatively reduced in the newly designed nozzle according to the existed nozzle, particularly in the regions close to the orifice entrance. However, it

21

has been observed that the uniformity in the contour of velocity and pressure distribution along the orifice decreases. Additionally, as seen in the velocity distribution contour from the new design, the dead zones are much more than the old design. This will adversely affect the backflow resistance of the nozzle.

Many improved correlations exist in the literature regarding the minimum required pressure drop at the primary air distributor grid for fluidized bed combustion systems. It was also stated that the minimum required pressure drop at the primary air distributor, which is widely accepted for large-scale CFB boilers, should be greater than 3.6 kPa [18].

In the new nozzle design, the pressure drop was 2.9 kPa which is below the required minimum value of 3.6 kPa. This will reduce the flow homogeneity in the bed region. The combustion efficiency of the CFB boiler will also decrease, and increase the backflow risk. Therefore, in order to optimize the newly designed nozzle, the effect of orifice number and diameter change on pressure and velocity is discussed in the following section.

3.3 Effects of the orifice number and its diameter

The number of orifices and diameter sizes in the nozzle have an interrelationship with the orifice outlet velocity and pressure drop. As the orifice diameter gets smaller, the air outlet velocities will increase. The aerodynamic drag force exerted on the bed material by the orifice outlet velocity is directly proportional to the square of the velocity. This will increase the backflow resistance. At the same time, with the increase in flow velocity at the orifice outlet, turbulence and uniformity of bed material in the bed region will increase. Thus, fluidization and combustion efficiency in the CFB boiler increase. On the other hand, It has been stated that a velocity greater than 90 m/sec at

the orifice outlet poses a risk in terms of boiler operation such as, high rate attrition of the bed material and so negative adversely affect the fluidization [15]. In this study of optimization, 90 m/s flow velocity was accepted as the upper limit for orifice outlet. The orifice outlet velocity in the bell-type air nozzle of CTPP boiler is 61 m/s and assumed as the lower limit. Pressure loss and velocity outlet parameters are two important nozzle design criteria and inversely proportional to each other. The pressure drop of 6.8 kPa in the CTPP boiler nozzle was accepted as the upper limit. As the lower limit value, the minimum required pressure drop of 3.6 kPa was accepted as recommended for large-scale CFB boilers in the literature. As a result, these limit values constitute the constraints for the optimization of the newly nozzle model. The effect of orifice numbers (4, 6, 8, 10 and 12) and diameter variables (12, 13, 14, 15,... and 26 mm) on the pressure drop and orifice outlet velocities in the newly nozzle model were investigated. Firstly, the flow volumes for each case were created in the 3D program in ANSYS SpaceClaim software. Afterwards, CFD analyzes were performed with FLUENT under CTPP boiler conditions for each model at 100% load. The pressure drop and orifice outlet velocity values obtained from CFD analyzes for each model are given in **Figs. 13.** and **14.** Accordingly, in order to determine the optimum orifice diameter regarding to the changing number of orifices in the nozzle, the intersection of the constraints defined separately in both figures was examined. As a result, it has been seen that there is an only one optimum orifice diameter size for each nozzle with 4, 6, 8, 10 and 12 orifices.
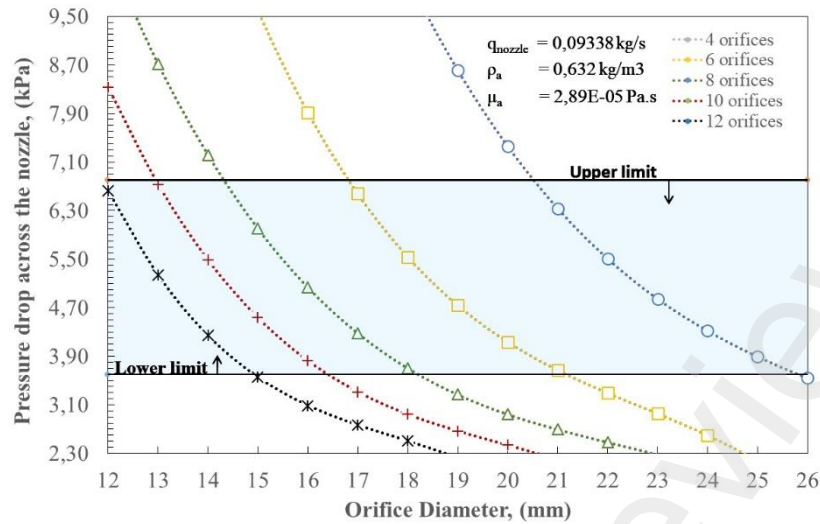
Fig. 13. Effect of orifice number and diameter variations on total pressure drop at the newly designed nozzle model.
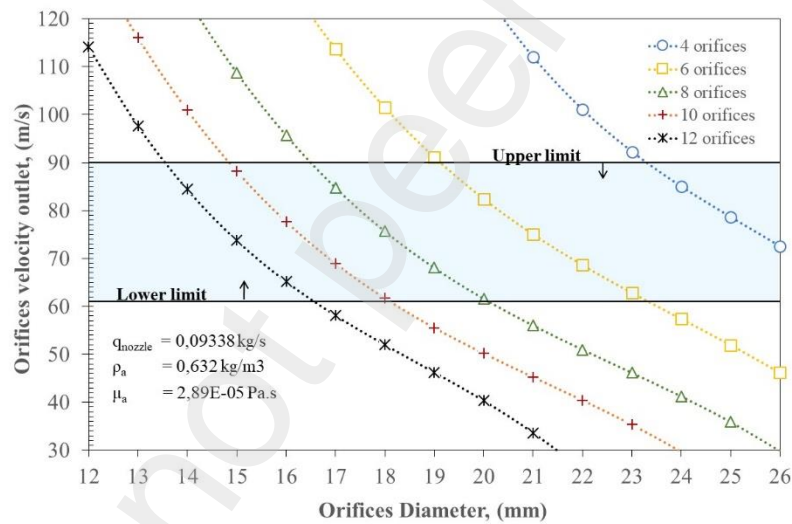

Fig. 14. Effect of orifice number and diameter variations on orifice velocity outlet at the newly designed nozzle model.

Pressure loss increases with the reduction of orifice diameters in the newly designed nozzle. Accordingly, when the number of orifices is 8 and the orifice diameter is 20 mm, the total pressure loss is 2.9 kPa, and when the same number of orifices and the orifice diameter is 17 mm, the total pressure loss is 4.2 kPa. For large scale CFB boilers, this value is greater than the minimum required pressure drop of 3.6 kPa at the primary air distributor plate and less than the pressure drop of 6.8 kPa for CTPP boiler

24

nozzles. Thus, internal energy consumption will be reduced. The orifice output velocity, 84.5 m/sec, is higher than the CTPP boiler nozzle, 61 m/s, and below the upper limit value of 90 m/sec. This will increase the combustion efficiency in the boiler and resistance to backflow of bed material. Similar pressure and velocity results will be seen for nozzles with 4, 6, 10, and 12 orifice numbers at the orifice diameters of 24, 20, 15, and 14mm, respectively.

Pressure and velocity distribution contours obtained as a result of CFD analyzes in optimum diameter depending on the number of orifices in the newly bell-type nozzle are given in **Figs. 15.** and **16.**
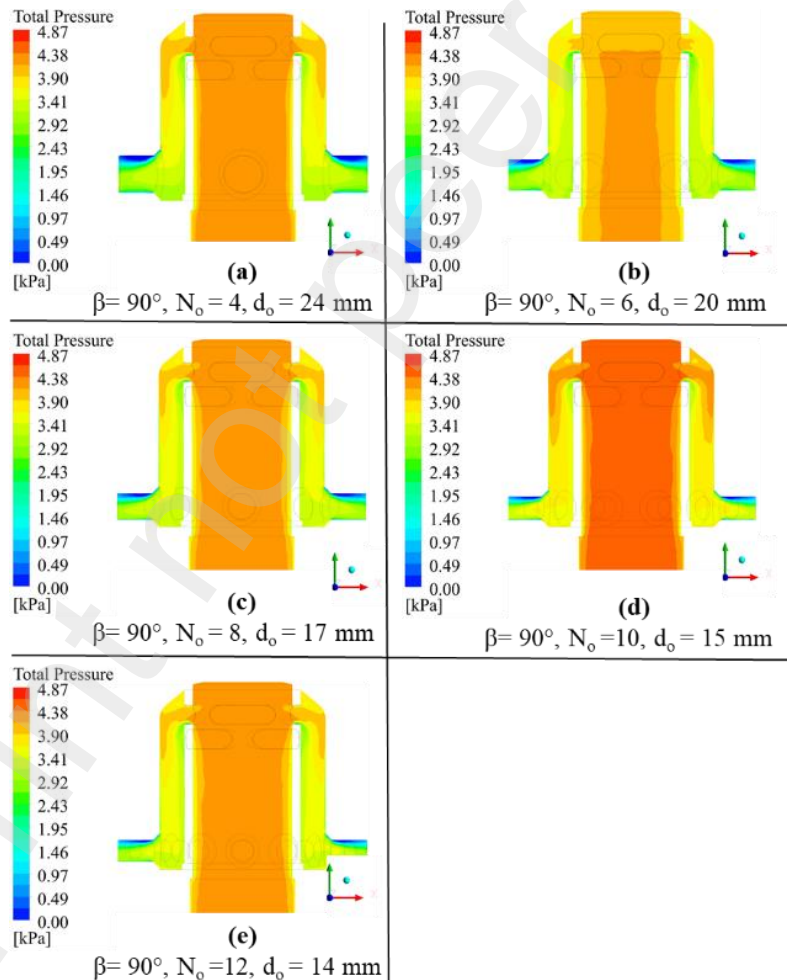

Fig. 15. Contours of the total pressure distribution at optimum orifice diameters regarding the varying number of orifices in the newly designed nozzle model.
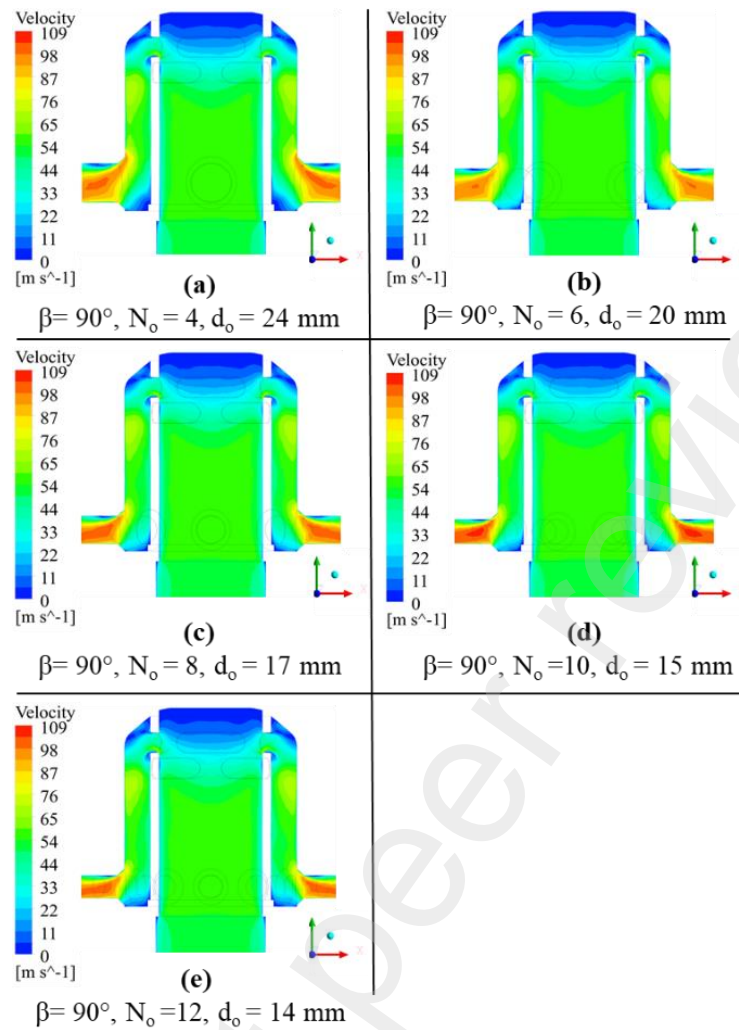
Fig. 16. Contours of the velocity distribution at optimum orifice diameters regarding the varying number of orifices in the newly designed nozzle model.

When these contours are examined, it can be seen that uniformity of pressure and velocity distribution, particularly at the orifices channels are decreased. Hence, there is a large amount of dead zone on the upper walls of the orifice channel. As a result, to increase the uniformity of pressure and velocity distribution in the orifice channel and to eliminate dead zones the effect of the orifice inclination angle is discussed in the following section.

26

3.4 Effects of the orifice angle

The inclination angle of the orifice on the nozzles should be between 90° and 135° with by the center tube [20]. In this study, the effect of orifice inclination angle on pressure and velocity distribution in the newly designed nozzle model was investigated. In this regard, 3D solid models of the nozzle at 90°, 105°, 120° and 135° orifice angles were designed. Additionally, in this section, the model with number of 8 orifices and 17 mm orifice diameter was taken as reference in the newly designed bell-type nozzle. The geometric views of the new nozzle model at four different orifice inclination angles are given in **Fig. 17.**
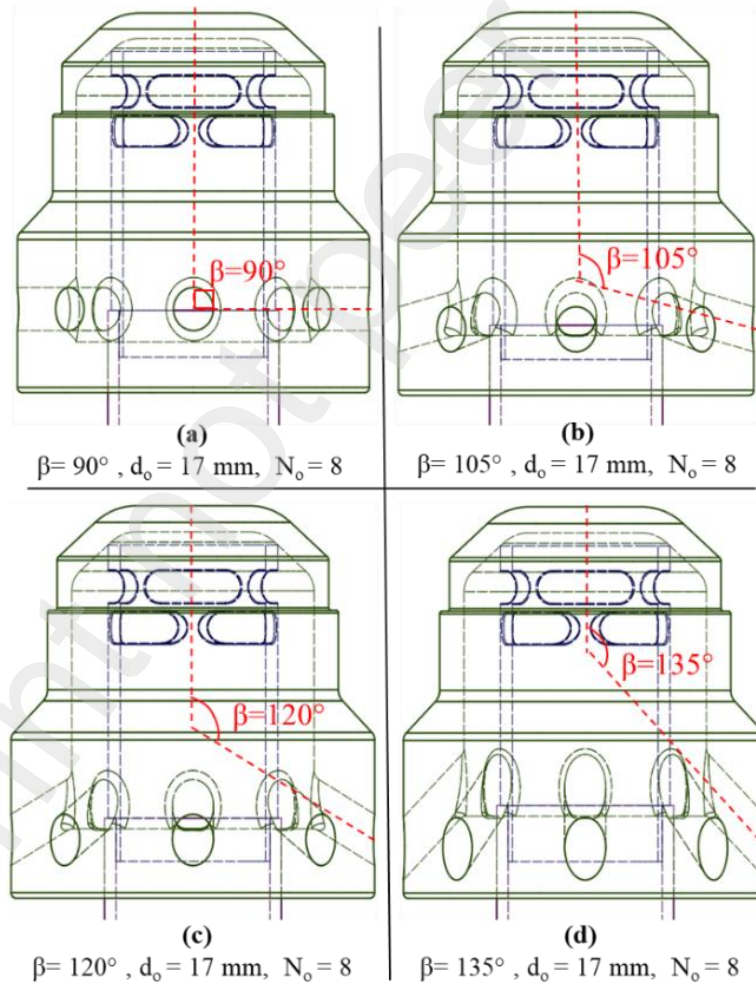

(a)
$\beta= 90°$, $d_o = 17$ mm, $N_o = 8$

(b)
$\beta= 105°$, $d_o = 17$ mm, $N_o = 8$

(c)
$\beta= 120°$, $d_o = 17$ mm, $N_o = 8$

(d)
$\beta= 135°$, $d_o = 17$ mm, $N_o = 8$

Fig. 17. Geometric view of the newly designed nozzle with 8 orifices and 17 mm orifice diameter at the four different orifice angles.

27

The effect of orifice angels (90°, 105°, 120° and 135°) and diameter variables (12, 13, 14, 15,… and 26 mm) on the pressure drop in the newly designed nozzle model were investigated. Within this scope, the pressure drop values obtained from CFD analyzes for each model are given in **Fig. 18**. According to this figure, the pressure loss decreased in the nozzle with the orifice inclination angle. For instance, in the nozzle with 8 orifices and 17 mm orifice diameter, when the orifice angle is 105° the total pressure drop is 3.95 kPa. However, with the increase of the inclination angle, that is, in the nozzles with 120° and 135° orifice inclination angle, the pressure loss remained nearly constant. In addition, with the increase of the nozzle orifice diameter, the effect of the inclination angle on the total pressure drop decreases.
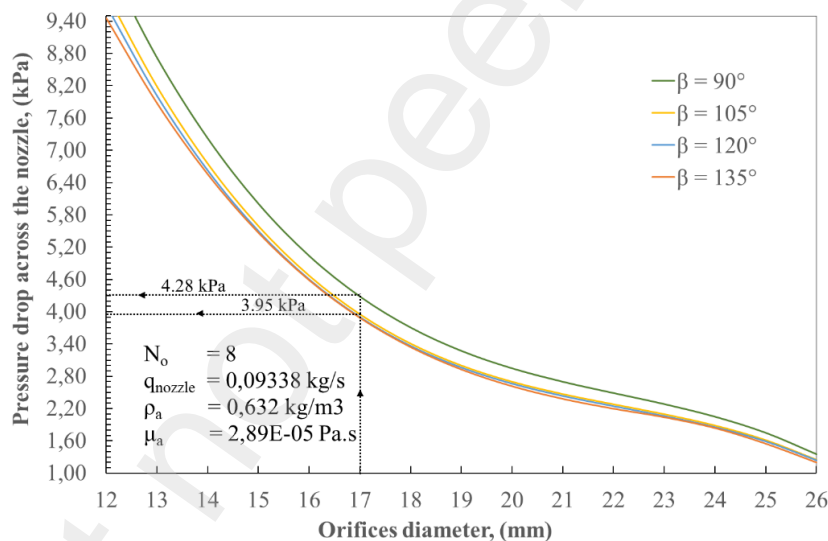

Fig. 18. Effect of orifice angel and diameter variations on total pressure drop at the newly designed nozzle model.

As for the effect of the orifice angle variations on total pressure drop and velocity distribution, the newly designed nozzle model with 8 orifices and 17 mm diameter was discussed at 90°, 105°, 120°, and 135° orifice angles. Accordingly, it was realized that the inclination angle of the orifice increased the total pressure and velocity distribution homogeneity and minimized the dead zones at the orifice channel as seen in **Fig. 19.**

28

and **Fig. 20.** However, when the velocity distribution contours are examined at the 120° and 145° orifice angles, seen the flow accelerates suddenly at the entrance of the orifice channel. This reduced the flow homogeneity at the orifice channel compared to the 105° orifice angle.
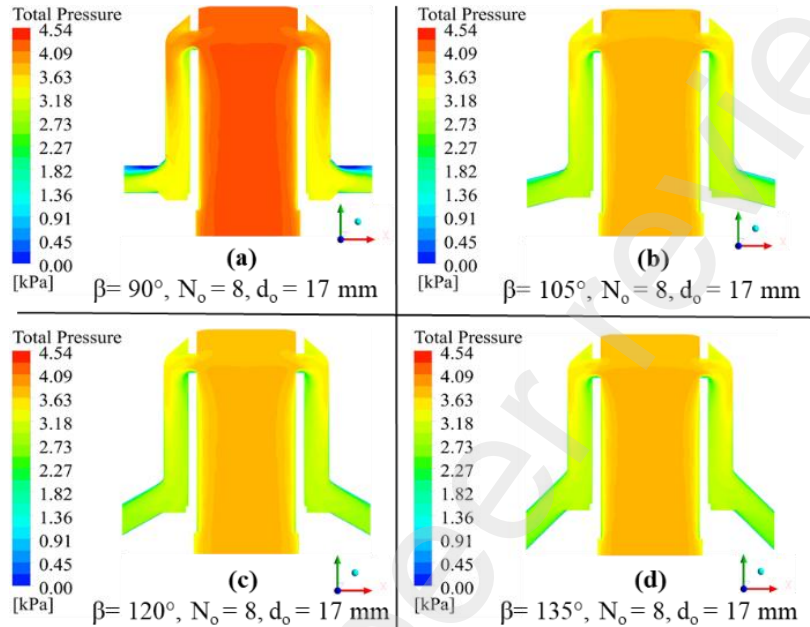

Fig. 19. Contours of total pressure distribution in newly designed nozzle model with the 8 orifices and 17 mm orifice diameter at the different orifice angles.
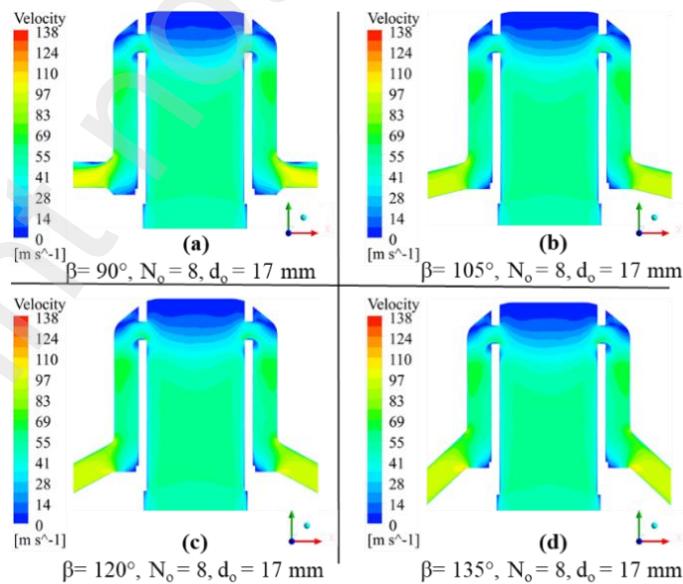

Fig. 20. Contours of velocity distribution in newly designed nozzle model with the 8 orifices and 17 mm orifice diameter at the different orifice angles.

In addition to the importance of homogeneity of the velocity distribution at the orifice channel, flow uniformity at the orifice velocity outlet is also important. Therefore, the uniformity index parameter defined in FLUENT was used to investigate the effects of orifice angle and diameter change on this parameter through CFD analysis. The uniformity index weighted by area represents how a velocity field variable varies over a surface, where a value of $\gamma_a = 1$ indicates the highest uniformity. In a nozzle, the uniformity air velocity is important to prevent reverse flow of the bed material at the orifice outlet. The effect of orifice angle and diameter changes on the uniformity index at the orifice outlet is as given in **Fig. 21**. Accordingly, as the uniform index ratio approaches 1, homogeneity increases at the orifice outlets. It can be seen that the uniformity index ratio of the orifice outlet increases when the inclination angle of the orifice is greater than 90° in the newly designed nozzle model with 8 orifices and 17 mm diameter. However, as the orifice inclined angle increased from 105°, the uniformity index ratio decreased. Additionally, as the orifice diameter increases, the effect of the inclination angle on the uniformity index ratio increases, but it tends to decrease. Finally, the best uniformity index ratio was obtained at the orifice angle of 105°, as in the velocity distribution contours analysis. Finally, the best uniformity index ratio was obtained at the orifice angle of 105° the same as in velocity distribution contours analysis. Accordingly, the uniformity index ratio at the orifice outlet for the 17 mm diameter is 0.963. Thus, the orifice inclined angle of 105° increased the uniformity index by about 2 % at the outlet of the orifices. This situation can increase the resistance of the nozzle to the backflow during CFB boiler operating.
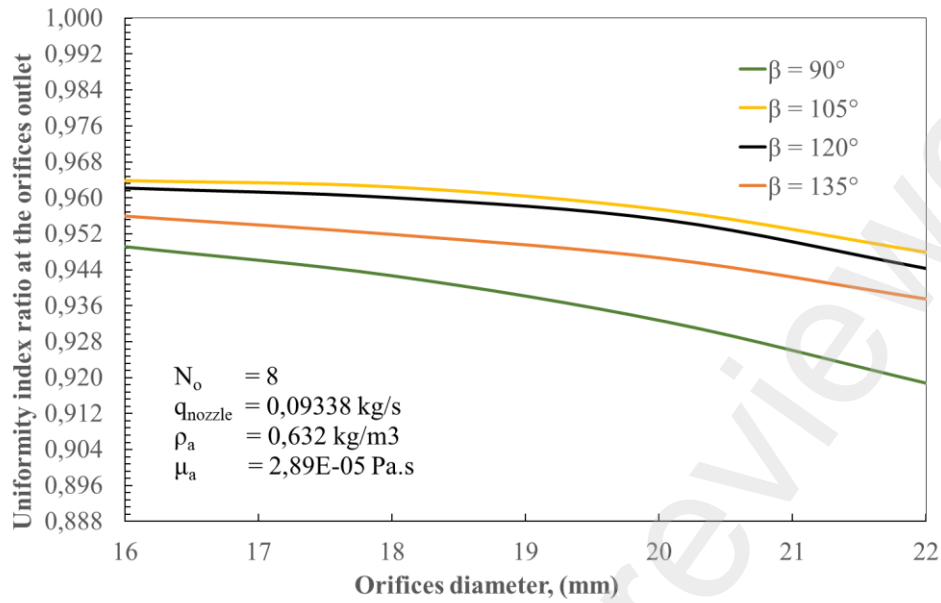
Fig. 21. Effect of orifice angel and diameter variations on the uniformity index at the orifice outlet at the newly designed nozzle model.

4. Results

This study investigated the optimization of bell-type primary air nozzle geometry according to pressure drop and outlet velocity at the orifices. Moreover, it was aimed to reduce the internal energy consumption of the CTPP boiler unit in this study by decreasing the pressure drop at the nozzle and improving the combustion efficiency and boiler operating efficiency aimed by increasing the velocties and uniformity index parameters at the orifices. All these studies were carried out with the help of CFD analysis.

Firstly, the pressure loss reduced from 6.81 kPa to 2.90 kPa by designing newly 8 slots instead of 16 holes in the nozzle inner head. Secondly, the orifice diameter was optimized based on the number of orifices. As the orifice diameter was optimized, the minimum required pressure drop at large-scale CFB boilers, 3,6 kPa, and the upper limit values of 90 m/s at the orifices velocity outlet were taken as constraints. Then, the angle of orifices at the nozzle was optimized according to contours of the velocity

31

and pressure distributions and uniformity index parameters at the orifice outlet through the CFD analysis.

The characteristic curve of the optimum newly designed and then optimized nozzle model is given **in Fig. 22.** Accordingly, at the boiler CTPP boiler operating full load, pressure drop at the nozzle and outlet velocity at the orifices occur respectively at 3.95 kPa and 84.4 m/s. Pressure loss and velocity outlet also decrease depending on the boiler operating load such as, at 85% and 50% loads in the CTPP's boiler. As the primary airflow rate remains constant when the boiler load operates below the 50% load, the pressure loss and velocity outlet are not changed.
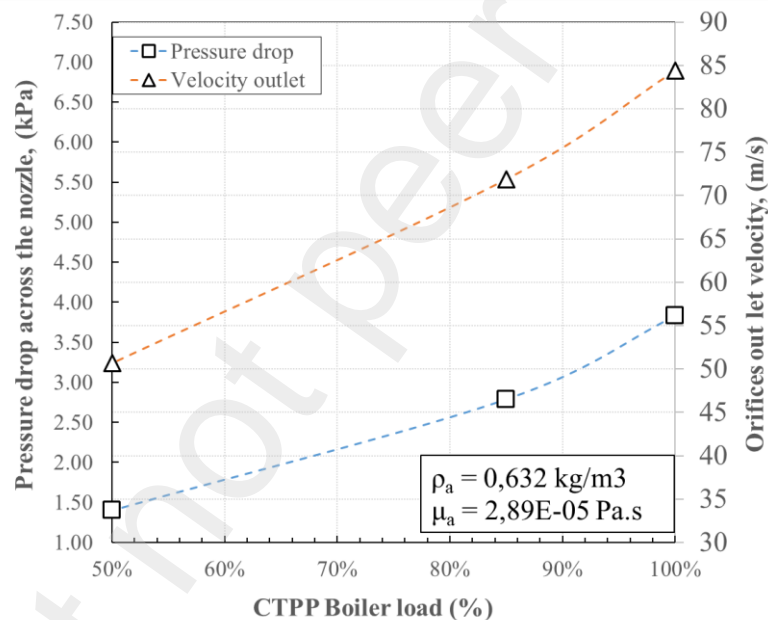

Fig. 22. Characteristic curve of the for newly designed bell-type air nozzle with the eight orifices, 17 mm orifice diameter and angel of orifice 105°.

The characteristic curve for the newly designed nozzle model with eight orifices at the 105° orifice angle is going to be almost similar for 4, 6, 10, and 12 orifices each of which has 24, 20, 15, and 14 mm diameters, respectively. The number of orifices and the diameter may vary depending on the designer's preference and ease of manufacture.

32

5. Conclusion

The newly designed and then optimized bell-type nozzle model with 8 orifices 17 mm diameter, 105 orifice angle decreased pressure drop from 6.81 kPa to 3.95 kPa. Thus, the energy consumption in primary fans by 14.56% will decrease and save 2.26 GWh/year in internal electricity consumption at the CTPP unit at the full load. In addition, with the newly designed nozzle model achieved uniform velocity distribution at the orifice channel and outlets, we eliminated the dead zones there and decreased the backflow of the bed materials risk in CTPP boiler operation. Moreover, it has been determined that orifices above the 105° angle are not a remarkable benefit in terms of pressure drop and velocity profile at the newly designed bell-type primary nozzle.

33

References

[1] Yue G, Cai R, Lu J, Zhang H. From a CFB reactor to a CFB boiler – The review of R&D progress of CFB coal combustion technology in China. Powder Technology 2017; 316:18–28. https://doi.org/10.1016/j.powtec.2016.10.062.

[2] Li PW, Chyang CS, Ni HW. An experimental study of the effect of nitrogen origin on the formation and reduction of NOx in fluidized-bed combustion. Energy 2018; 154:319–27. https://doi.org/10.1016/j.energy.2018.04.141.

[3] Ke X, Engblom M, Yang H, Brink A, Lyu JF, Zhang M, et al. Prediction and minimization of NOx emission in a circulating fluidized bed combustor: A comprehensive mathematical model for CFB combustion. Fuel 2022;309:122133. https://doi.org/10.1016/j.fuel.2021.122133.

[4] Arjunwadkar A, Basu P, Acharya B. A review of some operation and maintenance issues of CFBC boilers. Appl. Therm. Eng. 2016; 102:672–94. https://doi.org/10.1016/j.applthermaleng.2016.04.008.

[5] Cheng L, Ji J, Wei Y, Wang Q, Fang M, Luo Z, Ni M, Cen K. A note on large-size super-critical CFB technology development. Powder Technology 2020; 363:398–407. https://doi.org/10.1016/j.powtec.2019.12.044.

[6] Huang Z, Deng L, Che D. Development and technical progress in large-scale circulating fluidized bed boiler in China. Front Energy 2020; 14:699–714. https://doi.org/10.1007/s11708-020-0666-3.

[7] Basu P, Nag PK. Heat transfer to walls of a circulating fluidized-bed furnace. Chem Eng Sci 1996; 51:1–26. https://doi.org/10.1016/0009-2509(95)00124-7.

[8] Sobrino C, Ellis N, de Vega M. Distributor effects near the bottom region of turbulent fluidized beds. Powder Technology 2009; 189:25–33. https://doi.org/10.1016/j.powtec.2008.05.012.

[9] Kafle I, Bhochhibhoya S, Paudel L, Parajuli P, Prajapati S, Shrestha PL. Design and analysis of air distributors and bed materials of fluidized bed boiler. International Journal of Fluid Mechanics & Thermal Sciences 2016; 2:22-36. https://doi.org/10.11648/j.ijfmts.20160204.11.

[10] Guo Q, Werther J, Hartge E-U. Investigation into maldistribution in a circulating fluidized bed. China Particuology 2003;1:145–50. https://doi.org/10.1016/s1672-2515(07)60131-6.

[11] Shukrie A, Anuar S, Oumer AN. Air distributor designs for fluidized bed combustors: A Review. Engineering, Technology & Applied Science Research 2016; 6:1029–1034. https://doi.org/10.48084/etasr.688.

[12] Shenastaghi FK, Roshdi S, Kasiri N, Khanof MH. CFD simulation and experimental validation of bubble cap tray hydrodynamics. Separation and Purification Technology 2018; 192:110–122. https://doi.org/10.1016/j.seppur.2017.09.055.

[13] Vakhshouri K, Grace JR. Effects of the plenum chamber volume and distributor geometry on fluidized bed hydrodynamics. Particuology 2010;8:2–12. https://doi.org/10.1016/J.PARTIC.2009.05.005.

[14] Kunii D, Levenspiel O. Fluidization engineering. 2nd ed. Butterworth-Heinemann 1991. https://doi.org/10.1016/C2009-0-24190-0.

[15] Basu P. Circulating Fluidized Bed Boilers Design. 1th ed. Springer Cham 2015. https://doi.org/10.1007/978-3-319-06173-3.

[16] Yang HR, Huang ZM, Yue GX, Lu JF. Characteristics of a float nozzle designed for circulating fluidized bed boilers. Chemical Engineering & Technology 2007;30:1398–1400. https://doi.org/10.1002/ceat.200700044.

[17] Huang ZM, Yang HR, Liu Q, Wang Y, Lu JF, Yue GX. Characteristics of a modified bell jar nozzle designed for CFB boilers. Proceedings of the 20th International Conference on Fluidized Bed Combustion 2010; 492–495. https://doi.org/10.1007/978-3-642-02682-9_75.

[18] Mirek P. Designing of primary air nozzles for large-scale CFB boilers in a combined numerical-experimental approach. Chemical Engineering and Processing: Process Intensification 2011; 50:694–701. https://doi.org/10.1016/j.cep.2011.04.006.

[19] Omer A, Weng M. Effect of primary air maldistribution due to nozzle wear on CFBC performance. Fuel Processing Technology 2018; 173:191–196. https://doi.org/10.1016/j.fuproc.2017.12.008.

[20] Mirek P, Klajny M. Air nozzle design criteria for protection against the backflow of solids in CFB boilers. Applied Thermal Engineering 2018; 141:503–515. https://doi.org/10.1016/j.applthermaleng.2018.06.006.

[21]Liu X, Zhu G, Asim T, Zhang Y, Mishra R. The innovative design of air caps for improving the thermal efficiency of CFB boilers. Energy 2021; 221:119844. https://doi.org/10.1016/j.energy.2021.119844.

[22] Huang Z, Deng L, Che D. Experimental and CFD simulation studies on bell-type air nozzles of CFB boilers. Applied Sciences 2019; 9: 3805. https://doi.org/10.3390/app9183805.

[23] Mirek P. Experimental investigation of the flow characteristics of low-pressure drop air nozzles working with CFB boilers. E3S Web of Conferences 2019; 82. https://doi.org/10.1051/e3sconf/20198201013.

[24]Açikgöz B, Çelik C, Soyhan HS, Gökalp B, Karabaı B. Emission characteristics of an hydrogen–CH4 fuelled spark ignition engine. Fuel 2015; 159:298–307.

35

https://doi.org/10.1016/j.fuel.2015.06.043.

[25] Gocmen K, Soyhan HS. An intake manifold geometry for enhancement of pressure drop in a diesel engine. Fuel 2020; 261:116193. https://doi.org/10.1016/j.fuel.2019.116193.

[26] Oktay Z. Investigation of coal-fired power plants in Turkey and a case study: Can plant. Applied Thermal Engineering 2009; 29:550–557. https://doi.org/10.1016/j.applthermaleng.2008.03.025.

[27] Gürel B. Designing particle and water natural circulation system for combustion low quality lignite in the circulating fluidized bed boiler (CFBB) and investigation of the combustion characteristics (Ph.D. Thesis). Süleyman Demirel University, Institute of Science and Technology 2018.

[28] Zhang H, Tang S, Yue H, Wu K, Zhu Y, Liu C, Liang B, Li C. Comparison of computational fluid dynamic simulation of a stirred tank with polyhedral and tetrahedral meshes. Iranian Journal of Chemistry and Chemical Engineering 2020;39:311–319. https://doi.org/10.30492/ijcce.2019.34950.

[29] Çengel YA, Cimbala JM. Fluid Mechanics Fundamentals and Applications. 4th ed. McGraw-Hill Education 2018.

[30] Ji X, Lu X, Kang Y, Wang Q, Chen J. Design optimization of the bell type blast cap employed in small scale industrial circulating fluidized bed boilers. Advanced Powder Technology 2014; 25:281–291. https://doi.org/10.1016/j.apt.2013.04.016.

[31] Ansys I. Ansys Fluent Theory Guide. In: Ansys I, ed. 15.0 ed. The United States of America; 2013.

[32] Ahsan M. Numerical analysis of friction factor for a fully developed turbulent flow using k–ε turbulence model with enhanced wall treatment. Beni-Suef University Journal of Basic and Applied Sciences 2014; 3:269–277. https://doi.org/10.1016/j.bjbas.2014.12.001.

[33] Ngo TT, Go J, Zhou T, Nguyen VH, Lee GS. Enhancement of exit flow uniformity by modifying the shape of a gas torch to obtain a uniform temperature distribution on a steel plate during preheating. Applied Sciences 2018; 8:2197. https://doi.org/10.3390/app8112197.

36

Figure Captions

Fig. 1. Schematic diagram and characteristic parameters of the CFB boiler 160 MWe in CTPP.

Fig. 2. Schematic diagram of the primary airflow in the CTPP boiler bed zone.

Fig. 3. Schematic and configuration view of the bell-type nozzle in CTPP boiler.

Fig. 4. Boundary definitions in the nozzle airflow volume.

Fig. 5. Mesh independence study of the bell-type nozzle.

Fig. 6. Polyhedral meshing of the flow volume with ten inflation layers around orifices.

Fig. 7. Variation and average of total pressure drop across the nozzles in the CTPP

boiler.

Fig. 8. Characteristic curve of the existed bell-type nozzle.

Fig. 9. Variation of fan power consumption regarding pressure drop across the nozzle.

Fig. 10. Geometric view of the existed and newly designed bell-type nozzle.

Fig. 11. Contours of total pressure distribution (a) existing nozzle in CTPP Boiler (100% load); (b) newly designed nozzle model (100%load).

Fig. 12. Contours of velocity distribution (a) existing nozzle in CTPP Boiler (100% load); (b) newly designed nozzle model (100%load).

Fig. 13. Effect of orifice number and diameter variations on total pressure drop at the newly designed nozzle model.

Fig. 14. Effect of orifice number and diameter variations on orifice velocity outlet at the newly designed nozzle model.

Fig. 15. Contours of the total pressure distribution at optimum orifice diameters regarding the varying number of orifices in the newly designed nozzle model.

Fig. 16. Contours of the velocity distribution at optimum orifice diameters regarding the varying number of orifices in the newly designed nozzle model.

Fig. 17. Geometric view of the newly designed nozzle with 8 orifices and 17 mm orifice diameter at the 4 different orifice angles.

Fig. 18. Effect of orifice angel and diameter variations on total pressure drop at the newly designed nozzle model.

Fig. 19. Contours of total pressure distribution in newly designed nozzle model with the 8 orifices and 17 mm orifice diameter at the different orifice angles.

Fig. 20. Contours of velocity distribution in newly designed nozzle model with the 8 orifices and 17 mm orifice diameter at the different orifice angles.

Fig. 21. Effect of orifice angel and diameter variations on the uniformity index at the orifice outlet at the newly designed nozzle model.

Fig. 22. Characteristic curve of the for newly designed bell-type air nozzle with the eight orifices, 17 mm orifice diameter and angel of orifice 105°.

38